Measurement of the #[subscript c](1S) production cross-section in proton–proton collisions via the decay #[subscript c](1S) → p[bar over p]

Eur. Phys. J. C (2015) 75:311
DOI 10.1140/epjc/s10052-015-3502-x

THE EUROPEAN PHYSICAL JOURNAL C

Regular Article - Experimental Physics

Measurement of the $\eta_c(1S)$ production cross-section in proton–proton collisions via the decay $\eta_c(1S) \to p\overline{p}$

LHCb Collaboration[⋆]

CERN, 1211 Geneva 23, Switzerland

Received: 16 September 2014 / Accepted: 4 June 2015

Abstract The production of the $\eta_c(1S)$ state in proton-proton collisions is probed via its decay to the $p\overline{p}$ final state with the LHCb detector, in the rapidity range $2.0 < y < 4.5$ and in the meson transverse-momentum range $p_{\rm T} > 6.5\,{\rm GeV}/c$. The cross-section for prompt production of $\eta_c(1S)$ mesons relative to the prompt J/ψ cross-section is measured, for the first time, to be $\sigma_{\eta_c(1S)}/\sigma_{J/\psi} = 1.74 \pm 0.29 \pm 0.28 \pm 0.18_{\mathcal{B}}$ at a centre-of-mass energy $\sqrt{s} = 7$ TeV using data corresponding to an integrated luminosity of 0.7 fb^{-1}, and $\sigma_{\eta_c(1S)}/\sigma_{J/\psi} = 1.60 \pm 0.29 \pm 0.25 \pm 0.17_{\mathcal{B}}$ at $\sqrt{s} = 8$ TeV using 2.0 fb^{-1}. The uncertainties quoted are, in order, statistical, systematic, and that on the ratio of branching fractions of the $\eta_c(1S)$ and J/ψ decays to the $p\overline{p}$ final state. In addition, the inclusive branching fraction of b-hadron decays into $\eta_c(1S)$ mesons is measured, for the first time, to be $\mathcal{B}(b \to \eta_c X) = (4.88 \pm 0.64 \pm 0.29 \pm 0.67_{\mathcal{B}}) \times 10^{-3}$, where the third uncertainty includes also the uncertainty on the J/ψ inclusive branching fraction from b-hadron decays. The difference between the J/ψ and $\eta_c(1S)$ meson masses is determined to be $114.7 \pm 1.5 \pm 0.1$ MeV/c^2.

1 Introduction

High centre-of-mass energies available in proton-proton collisions at the LHC allow models describing charmonium production to be tested. We distinguish promptly produced charmonia from those originating from b-hadron decays. Promptly produced charmonia include charmonia directly produced in parton interactions and those originating from the decays of heavier quarkonium states, which are in turn produced in parton interactions. While measurements of J/ψ and $\psi(2S)$ meson production rates at the LHC [1–6] are successfully described by next-to-leading order (NLO) calculations in non-relativistic quantum chromodynamics (QCD) [7], the observation of small or no polarization in J/ψ meson prompt production [2] remains unexplained within the available theoretical framework [8]. The investigation of the lowest state, the $\eta_c(1S)$ meson, can provide important additional information on the long-distance matrix elements [9,10]. In particular, the heavy-quark spin-symmetry relation between the $\eta_c(1S)$ and J/ψ matrix elements can be tested, with the NLO calculations predicting a different dependence of the production rates on charmonium transverse momentum, $p_{\rm T}$, for spin singlet ($\eta_c(1S)$) and triplet (J/ψ, χ_{cJ}) states [11–13]. Thus, a measurement of the $p_{\rm T}$ dependence of the $\eta_c(1S)$ production rate, in particular in the low $p_{\rm T}$ region, can have important implications. Recent LHCb results on prompt production of χ_c states [14] provide information on the production of the P-wave states χ_{c0} and χ_{c2} at low $p_{\rm T}$, using the well-understood χ_{c1} production as a reference. A measurement of the cross-section of prompt $\eta_c(1S)$ production may allow an important comparison with the χ_{c0} results and yields indirect information on the production of heavier states.

At LHC energies, all b-hadron species are produced, including weakly decaying B^-, $\overline{B}^0$, $\overline{B}^0_{\rm s}$, B_c^- mesons, b-baryons, and their charge-conjugate states. A previous study of inclusive $\eta_c(1S)$ meson production in b-hadron decays by the CLEO experiment, based on a sample of B^- and $\overline{B}^0$ mesons, placed an upper limit on the combined inclusive branching fraction of B^- and $\overline{B}^0$ meson decays into final states containing an $\eta_c(1S)$ meson of $\mathcal{B}(B^-, \overline{B}^0 \to \eta_c(1S)X) < 9 \times 10^{-3}$ at 90 % confidence level [15]. Exclusive analyses of $\eta_c(1S)$ and J/ψ meson production in b-hadron decays using the $B \to K(p\overline{p})$ decay mode have been performed by the BaBar experiment [16], by the Belle experiment [17] and recently by the LHCb experiment [18].

In the present paper we report the first measurement of the cross-section for the prompt production of $\eta_c(1S)$ mesons in pp collisions at $\sqrt{s} = 7$ TeV and $\sqrt{s} = 8$ TeV centre-of-mass energies, as well as the b-hadron inclusive branching fraction into $\eta_c(1S)$ final states. This paper extends the scope of previous charmonium production studies reported by LHCb, which were restricted to the use of J/ψ or

⋆ e-mail: sergey.barsuk@cern.ch

Published online: 04 July 2015

$\psi(2S)$ decays to dimuon final states [1,2,14,19]. In order to explore states that do not have $J^{PC} = 1^{--}$ quantum numbers, while avoiding reconstruction of radiative decays with low-energy photons, the authors of Ref. [20] suggested to investigate hadronic final states. In the present analysis, we reconstruct $\eta_c(1S)$ mesons decaying into the $p\overline{p}$ final state. All well-established charmonium states decay to $p\overline{p}$ final states [20,21]. With its powerful charged-hadron identification and high charmonium production rate, the LHCb experiment is well positioned for these studies. The measurements are performed relative to the topologically and kinematically similar $J/\psi \to p\overline{p}$ channel, which allows partial cancellation of systematic uncertainties in the ratio. This is the first such inclusive analysis using decays to hadronic final states performed at a hadron collider.

In addition, a departure in excess of two standard deviations between the recent BES III results [22,23] and earlier measurements [21] motivates the determination of the difference between J/ψ and $\eta_c(1S)$ meson masses $\Delta M_{J/\psi,\,\eta_c(1S)} \equiv M_{J/\psi} - M_{\eta_c(1S)}$ using a different technique and final state. In the present analysis, the low-background sample of charmonia produced in b-hadron decays is used to determine $\Delta M_{J/\psi,\,\eta_c(1S)}$ and the $\eta_c(1S)$ natural width, $\Gamma_{\eta_c(1S)}$.

In Sect. 2 we present the LHCb detector and data sample used for the analysis. Section 3 describes the analysis details, while the systematic uncertainties are discussed in Sect. 4. The results are given in Sect. 5 and summarized in Sect. 6.

2 LHCb detector and data sample

The LHCb detector [24] is a single-arm forward spectrometer covering the pseudorapidity range $2 < \eta < 5$, designed for the study of particles containing b or c quarks. The detector includes a high-precision tracking system consisting of a silicon-strip vertex detector surrounding the pp interaction region, a large-area silicon-strip detector located upstream of a dipole magnet with a bending power of about 4 Tm, and three stations of silicon-strip detectors and straw drift tubes placed downstream of the magnet. The combined tracking system provides a momentum measurement with a relative uncertainty that varies from 0.4 % at low momentum to 0.6 % at 100 GeV/c, and an impact parameter measurement with a resolution of 20 μm for charged particles with large transverse momentum. Different types of charged hadrons are distinguished using information from two ring-imaging Cherenkov detectors. Photon, electron, and hadron candidates are identified by a system consisting of scintillating-pad and preshower detectors, an electromagnetic calorimeter, and a hadronic calorimeter. Muons are identified by a system composed of alternating layers of iron and multiwire proportional chambers. The trigger consists of a hardware stage, based on information from the calorimeter and muon systems, followed by a software stage, which applies a full event reconstruction.

Events enriched in signal decays are selected by the hardware trigger, based on the presence of a single high-energy deposit in the calorimeter. The subsequent software trigger specifically rejects high-multiplicity events and selects events with two oppositely charged particles having good track-fit quality and transverse momentum larger than 1.9 GeV/c. Proton and antiproton candidates are identified using the information from Cherenkov and tracking detectors [25]. Selected p and $\overline{p}$ candidates are required to form a good quality vertex. In order to further suppress the dominant background from accidental combinations of random tracks (combinatorial background), charmonium candidates are required to have high transverse momentum, $p_{\rm T} > 6.5$ GeV/c.

The present analysis uses pp collision data recorded by the LHCb experiment at $\sqrt{s} = 7$ TeV, corresponding to an integrated luminosity of 0.7 fb^{-1}, and at $\sqrt{s} = 8$ TeV, corresponding to an integrated luminosity of 2.0 fb^{-1}.

Simulated samples of $\eta_c(1S)$ and J/ψ mesons decaying to the $p\overline{p}$ final state, and J/ψ decaying to the $p\overline{p}\pi^0$ final state, are used to estimate efficiency ratios, the contribution from the decay $J/\psi \to p\overline{p}\pi^0$, and to evaluate systematic uncertainties. In the simulation, pp collisions are generated using Pythia [26] with a specific LHCb configuration [27]. Decays of hadronic particles are described by EvtGen [28], in which final-state radiation is generated using Photos [29]. The interaction of the generated particles with the detector and its response are implemented using the Geant4 toolkit [30,31] as described in Ref. [32].

3 Signal selection and data analysis

The signal selection is largely performed at the trigger level. The offline analysis, in addition, requires the transverse momentum of p and $\overline{p}$ to be $p_{\rm T} > 2.0$ GeV/c, and restricts charmonium candidates to the rapidity range $2.0 < y < 4.5$.

Discrimination between promptly produced charmonium candidates and those from b-hadron decays is achieved using the pseudo-decay time $t_z = \Delta z \cdot M/p_z$, where Δz is the distance along the beam axis between the corresponding pp collision vertex (primary vertex) and the candidate decay vertex, M is the candidate mass, and p_z is the longitudinal component of its momentum. Candidates with $t_z < 80$ fs are classified as prompt, while those with $t_z > 80$ fs are classified as having originated from b-hadron decays. For charmonium candidates from b-hadron decays, a significant displacement of the proton tracks with respect to the primary vertex is also required.

The selected samples of prompt charmonium candidates and charmonia from b-hadron decays have some candidates wrongly classified (cross-feed). The cross-feed probability is estimated using simulated samples and is scaled using the observed signal candidate yields in data. The cross-feed component is subtracted to obtain the ratio of produced $\eta_c(1S)$ and J/ψ mesons decaying into the $p\overline{p}$ final state. Corrections range from 2 % to 3 % for the ratio of promptly produced $\eta_c(1S)$ and J/ψ mesons, and from 8 % to 10 % for the ratio of charmonia produced in b-hadron decays.

The ratios of signal yields are expressed in terms of ratios of cross-sections multiplied by the decay branching fractions as

$$\frac{N^P_{\eta_c(1S)}}{N^P_{J/\psi}} = \frac{\sigma(\eta_c(1S)) \times \mathcal{B}(\eta_c(1S)\to p\overline{p})}{\sigma(J/\psi) \times \mathcal{B}(J/\psi\to p\overline{p})},$$

$$\frac{N^b_{\eta_c(1S)}}{N^b_{J/\psi}} = \frac{\mathcal{B}(b\to \eta_c(1S)X) \times \mathcal{B}(\eta_c(1S)\to p\overline{p})}{\mathcal{B}(b\to J/\psi X) \times \mathcal{B}(J/\psi\to p\overline{p})},$$

where N^P and N^b are the numbers of charmonia from prompt production and b-hadron decays, respectively. The simulation describes the kinematic-related differences between the $\eta_c(1S)$ and J/ψ decay modes reasonably well and predicts that the relative efficiencies for selecting and reconstructing $\eta_c(1S)$ and J/ψ mesons differ by less than 0.5%. Equal efficiencies are assumed for the $\eta_c(1S)$ and J/ψ meson reconstruction and selection criteria. The efficiency for selecting and reconstructing prompt J/ψ mesons is corrected for polarization effects, as a function of rapidity and p_{T}, according to Ref. [2].

The numbers of reconstructed $\eta_c(1S)$ and J/ψ candidates are extracted from an extended maximum likelihood fit to the unbinned $p\overline{p}$ invariant mass distribution. The J/ψ peak position $M_{J/\psi}$ and the mass difference $\Delta M_{J/\psi,\eta_c(1S)}$ are fitted in the sample of charmonia from b-hadron decays, where the signal is more prominent because of the reduced background level due to charmonium decay-vertex displacement requirements. The results are then used to apply Gaussian constraints in the fit to the $p\overline{p}$ invariant mass spectrum in the prompt production analysis, where the signal-to-background ratio is smaller, due to large combinatorial backgrounds.

The signal shape is defined by the detector response, combined with the natural width in the case of the $\eta_c(1S)$ resonance. The detector response is described using two Gaussian functions with a common mean value. In the description of each resonance, the ratio of narrow to wide Gaussian widths, $\sigma^a_{J/\psi}/\sigma^b_{J/\psi} = \sigma^a_{\eta_c(1S)}/\sigma^b_{\eta_c(1S)}$, the fraction of the narrow Gaussian component, and the ratio of the $\eta_c(1S)$ and J/ψ narrow Gaussian widths, $\sigma^a_{\eta_c(1S)}/\sigma^a_{J/\psi}$, are fixed in the fit to the values observed in simulation. The only resolution parameter left free in the fit to the low-background sample from b-hadron decays, $\sigma^a_{J/\psi}$, is fixed to its central value in the fit to the prompt sample. The natural width $\Gamma_{\eta_c(1S)}$ of the $\eta_c(1S)$ resonance is also extracted from the fit to the b-hadron decays sample, and is fixed to that value in the prompt production analysis. Gaussian constraints on the J/ψ meson mass and the $\Delta M_{J/\psi,\,\eta_c(1S)}$ mass difference from the fit to the b-hadron decays sample are applied in the prompt production analysis. The fit with free mass values gives consistent results.

The combinatorial background is parametrized by an exponential function in the fit of the sample from b-hadron decays, and by a third-order polynomial in the fit to the prompt sample.

Combinations of $p\overline{p}$ from the decay $J/\psi\to p\overline{p}\pi^0$ potentially affect the region close to the $\eta_c(1S)$ signal; hence, this contribution is specifically included in the background description. It produces a non-peaking contribution, and its mass distribution is described by a square-root shape to account for the phase space available to the $p\overline{p}$ system from the $J/\psi\to p\overline{p}\pi^0$ decay, convolved with two Gaussian functions to account for the detector mass resolution. In the fit to the $p\overline{p}$ invariant mass spectrum, the normalization of this contribution is fixed using the number of candidates found in the J/ψ signal peak and the ratios of branching fractions and efficiencies for the $J/\psi\to p\overline{p}\pi^0$ and $J/\psi\to p\overline{p}$ decay modes.

The $p\overline{p}$ invariant mass spectra for charmonium candidates from b-hadron decays in the 7 TeV and 8 TeV data are observed to be consistent. The two data samples are therefore combined and the resulting spectrum is shown in Fig. 1 with the fit overlaid.

The J/ψ meson signal is modelled using a double-Gaussian function. The $\eta_c(1S)$ signal is modelled using a relativistic Breit–Wigner function convolved with a double-Gaussian function. The background contribution from the $J/\psi\to p\overline{p}\pi^0$ decay with an unreconstructed pion, is small. The fit yields 2020 ± 230 $\eta_c(1S)$ signal decays and 6110 ± 116 J/ψ signal decays.

The results of the fit to the $p\overline{p}$ invariant mass spectrum of the prompt sample are shown in Fig. 2a and b for data collected at $\sqrt{s} = 7$ TeV and $\sqrt{s} = 8$ TeV, respectively. The fits yield $13\,370 \pm 2260$ $\eta_c(1S)$ and $11\,052 \pm 1004$ J/ψ signal decays for the data taken at $\sqrt{s} = 7$ TeV, and $22\,416\pm 4072$ $\eta_c(1S)$ and $20\,217 \pm 1403$ J/ψ signal decays for the $\sqrt{s} = 8$ TeV data.

In order to assess the quality of these unbinned fits to the invariant $p\bar{p}$ mass spectra, the chisquare per degree of freedom was calculated for the binning schemes shown in Figs. 1, and 2a, b. The values are 1.3, 1.7 and 1.8, respectively.

From the observed $\eta_c(1S)$ and J/ψ yields, and taking into account cross-feed between the samples, the yield ratios are obtained as

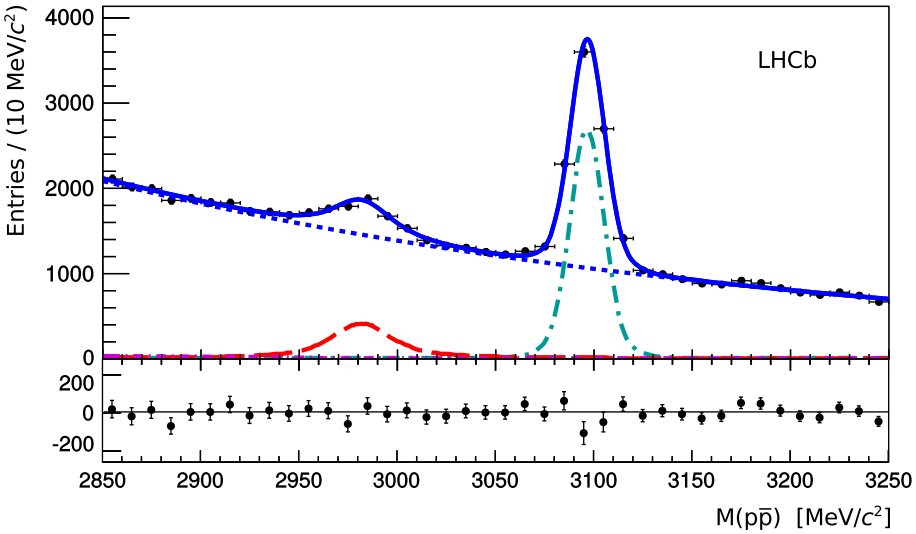

Fig. 1 Proton–antiproton invariant mass spectrum for candidates originating from a secondary vertex and reconstructed in $\sqrt{s} = 7$ TeV and $\sqrt{s} = 8$ TeV data. The *solid blue line* represents the best-fit curve, the *long-dashed red line* corresponds to the $\eta_c(1S)$ signal, the *dashed-dotted cyan line* corresponds to the J/ψ signal, and the *dashed magenta line* corresponds to the small contribution from $J/\psi \to p\bar{p}\pi^0$ decays with the pion unreconstructed. The *dotted blue line* corresponds to the combinatorial background. The distribution of the difference between data points and the fit function is shown in the *bottom panel*

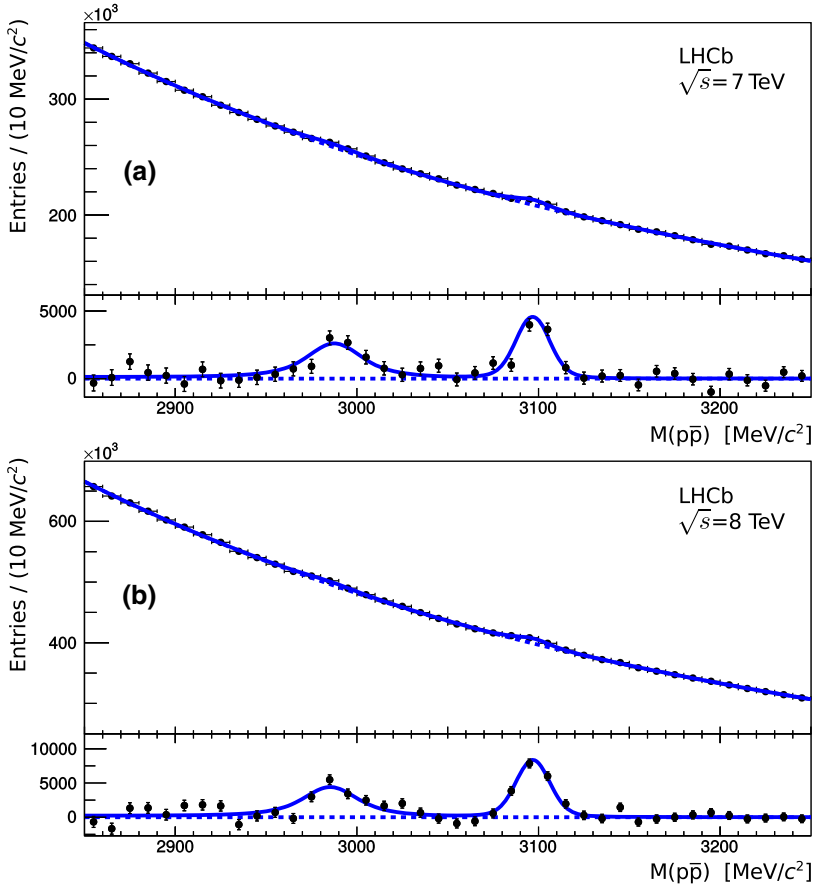

Fig. 2 Proton–antiproton invariant mass spectrum for candidates originating from a primary vertex (*upper panel* in each plot), and distribution of differences between data and the background distribution resulting from the fit (*lower panel* in each plot), in data at **a** $\sqrt{s} = 7$ TeV and **b** $\sqrt{s} = 8$ TeV centre-of-mass energies. Distributions on the *upper panels* are zero-suppressed

$$(N^P_{\eta_c(1S)}/N^P_{J/\psi})_{\sqrt{s}=7\ \text{TeV}} = 1.24 \pm 0.21,$$
$$(N^P_{\eta_c(1S)}/N^P_{J/\psi})_{\sqrt{s}=8\ \text{TeV}} = 1.14 \pm 0.21$$

and

$$N^b_{\eta_c(1S)}/N^b_{J/\psi} = 0.302 \pm 0.039$$

for the prompt production and charmonium production in b-hadron decays. Only statistical uncertainties are given in the above ratios.

4 Systematic uncertainties

We consider systematic uncertainties due to limited knowledge of the detector mass resolution, the J/ψ polarization, the $\eta_c(1S)$ natural width, possible differences of the prompt charmonium production spectra in data and simulation, cross-feed between the prompt charmonium sample and the charmonium sample from b-hadron decays, background description and feed-down from $J/\psi \to p\bar{p}\pi^0$ decays.

Uncertainties due to limited knowledge of the detector mass resolution are estimated by assigning the same σ^a value to the $\eta_c(1S)$ and J/ψ signal description for the b-hadron sample, and by varying the σ^a parameters in the prompt production analysis within their uncertainties. Uncertainties associated with the J/ψ polarization in the prompt production reflect those of the polarization measurement in Ref. [2]. We evaluate a potential contribution from J/ψ polarization in b-hadron decays using a BaBar study [32] of the J/ψ polarization in inclusive decays of B mesons. Simulations are used to estimate the effective polarization parameter for the LHCb kinematic region where the b-hadrons have a high boost and the longitudinal polarization is significantly reduced. A conservative value for the polarization parameter of -0.2 is used to estimate the corresponding systematic uncertainty. In order to estimate the systematic uncertainty associated with the $\eta_c(1S)$ natural width, which enters the results for the prompt production analysis, the world average $\Gamma_{\eta_c(1S)}$ value of 32.0 MeV from Ref. [21] is used. Possible differences of the prompt charmonium production spectra in data and simulation are estimated by correcting the efficiency derived from simulation according to the observed p_{T} distribution. The uncertainty related to the cross-feed is estimated by varying the signal yields in each sample according to their uncertainties. Uncertainties associated with the background description are estimated by using an alternative parametrization and varying the fit range. The uncertainty due to the contribution from the $J/\psi \to p\bar{p}\pi^0$ decay is dominated by the modelling of the $p\bar{p}$ invariant mass shape, and is estimated by using an alternative parametrization, which is linear instead of the square root. Possible systematic effect related to separation between prompt and b-decays samples, was checked by varying the t_z discriminant value from 80 to 120 fs. The results are found to be stable under variation of the value of the t_z discriminant, and no related systematic uncertainty is assigned. Table 1 lists the systematic uncertainties for the production yield ratio. The total systematic uncertainty is estimated as the quadratic sum of the uncertainties from the sources listed in Table 1 and, in the case of the prompt production measurement, is dominated by the uncertainty associated with the $\eta_c(1S)$ natural width. For the measurement with b-hadron decays the uncertainties associated with the background model, the J/ψ polarization and the cross-feed provide significant contributions.

Table 1 Summary of uncertainties for the yield ratio $N_{\eta_c(1S)}/N_{J/\psi}$

	Production in b-Hadron decays	Prompt production	
		$\sqrt{s} = 7$ TeV	$\sqrt{s} = 8$ TeV
Statistical uncertainty	0.039	0.21	0.21
Systematic uncertainties			
Signal resolution ratio (simulation)	0.006	0.04	0.03
Signal resolution variation		0.01	0.01
J/ψ polarization	0.009	0.02	0.02
$\Gamma_{\eta_c(1S)}$ variation		0.15	0.14
Prompt production spectrum	0.003	0.07	0.06
Cross-feed	0.008	0.01	0.01
Background model	0.011	0.09	0.09
Total systematic uncertainty	0.018	0.20	0.18

5 Results

The yield ratio for charmonium production in b-hadron decays is obtained as

$$N^b_{\eta_c(1S)}/N^b_{J/\psi} = 0.302 \pm 0.039 \pm 0.015.$$

In all quoted results, the first uncertainty refers to the statistical contribution and the second to the systematic contribution. By correcting the yield ratio with the ratio of branching fractions $\mathcal{B}(J/\psi \to p\bar{p})/\mathcal{B}(\eta_c(1S) \to p\bar{p}) = 1.39 \pm 0.15$ [21], the ratio of the inclusive b-hadron branching fractions into $\eta_c(1S)$ and J/ψ final states for charmonium transverse momentum $p_{\mathrm{T}} > 6.5\,\mathrm{GeV}/c$ is measured to be

$$\mathcal{B}(b \to \eta_c(1S)X)/\mathcal{B}(b \to J/\psi X) = 0.421 \pm 0.055 \pm 0.025 \pm 0.045_{\mathcal{B}},$$

where the third uncertainty is due to that on the $J/\psi \to p\bar{p}$ and $\eta_c(1S) \to p\bar{p}$ branching fractions [21]. Assuming that the $p_{\mathrm{T}} > 6.5\,\mathrm{GeV}/c$ requirement does not bias the distribution of charmonium momentum in the b-hadron rest frame, and

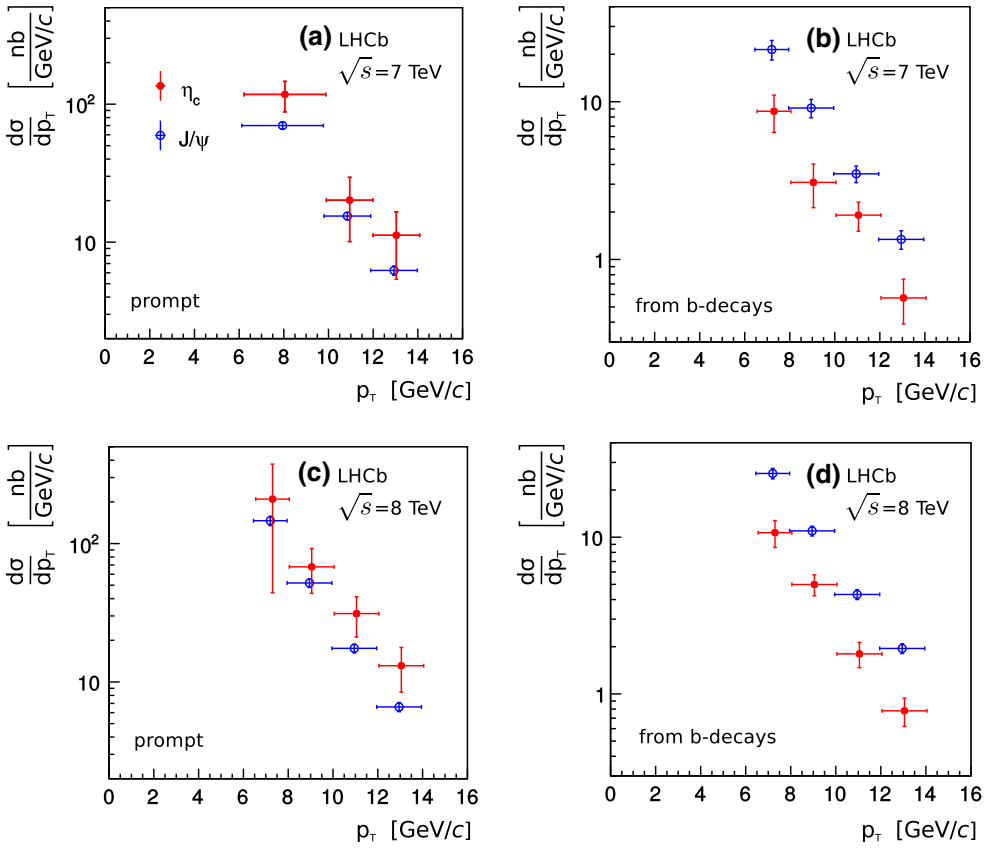

Fig. 3 Transverse momentum spectra for $\eta_c(1S)$ mesons (*red filled circles*). The p_{T} spectra of J/ψ from Refs. [1–3] are shown for comparison as *blue open circles*. Prompt production spectra are shown on **a** and **c** for data collected at $\sqrt{s} = 7$ TeV and $\sqrt{s} = 8$ TeV, respectively. The spectra from inclusive charmonium production in b-hadron decays are shown on **b** and **d** for data collected at $\sqrt{s} = 7$ TeV and $\sqrt{s} = 8$ TeV, respectively

using the branching fraction of b-hadron inclusive decays into J/ψ mesons from Ref. [21], $\mathcal{B}(b\to J/\psi X) = (1.16 \pm 0.10)\%$, the inclusive branching fraction of $\eta_c(1S)$ from b-hadron decays is derived as

$$\mathcal{B}(b\to\eta_c(1S)X) = (4.88 \pm 0.64 \pm 0.29 \pm 0.67_{\mathcal{B}}) \times 10^{-3},$$

where the third uncertainty component includes also the uncertainty on the J/ψ inclusive branching fraction from b-hadron decays. This is the first measurement of the inclusive branching fraction of b-hadrons to an $\eta_c(1S)$ meson. It is consistent with a previous 90 % confidence level upper limit restricted to B^- and $\overline{B}^0$ decays, $\mathcal{B}(B^-, \overline{B}^0\to\eta_c(1S)X) < 9 \times 10^{-3}$ [15].

The prompt production yield ratios at the different centre-of-mass energies are obtained as

$$(N^P_{\eta_c(1S)}/N^P_{J/\psi})_{\sqrt{s}=7\,\mathrm{TeV}} = 1.24 \pm 0.21 \pm 0.20,$$
$$(N^P_{\eta_c(1S)}/N^P_{J/\psi})_{\sqrt{s}=8\,\mathrm{TeV}} = 1.14 \pm 0.21 \pm 0.18.$$

After correcting with the ratio of branching fractions $\mathcal{B}(J/\psi\to p\overline{p})/\mathcal{B}(\eta_c(1S)\to p\overline{p})$ [21], the relative $\eta_c(1S)$ to J/ψ prompt production rates in the kinematic regime $2.0 < y < 4.5$ and $p_{\mathrm{T}} > 6.5\,\mathrm{GeV}/c$ are found to be

$$(\sigma_{\eta_c(1S)}/\sigma_{J/\psi})_{\sqrt{s}=7\,\mathrm{TeV}} = 1.74 \pm 0.29 \pm 0.28 \pm 0.18_{\mathcal{B}},$$

for the data sample collected at $\sqrt{s} = 7\,\mathrm{TeV}$, and

$$(\sigma_{\eta_c(1S)}/\sigma_{J/\psi})_{\sqrt{s}=8\,\mathrm{TeV}} = 1.60 \pm 0.29 \pm 0.25 \pm 0.17_{\mathcal{B}},$$

for the data sample collected at $\sqrt{s} = 8\,\mathrm{TeV}$. The third contribution to the uncertainty is due to that on the $J/\psi\to p\overline{p}$ and $\eta_c(1S)\to p\overline{p}$ branching fractions.

The absolute $\eta_c(1S)$ prompt cross-section is calculated using the J/ψ prompt cross-section measured in Refs. [2] and [3] and integrated in the kinematic range of the present analysis, $2.0 < y < 4.5$ and $p_{\mathrm{T}} > 6.5\,\mathrm{GeV}/c$. The corresponding J/ψ prompt cross-sections were determined to be $(\sigma_{J/\psi})_{\sqrt{s}=7\,\mathrm{TeV}} = 296.9 \pm 1.8 \pm 16.9\,\mathrm{nb}$ for $\sqrt{s} = 7\,\mathrm{TeV}$ [2], and $(\sigma_{J/\psi})_{\sqrt{s}=8\,\mathrm{TeV}} = 371.4 \pm 1.4 \pm 27.1\,\mathrm{nb}$ for $\sqrt{s} = 8\,\mathrm{TeV}$ [3]. The J/ψ meson is assumed to be produced unpolarized. The prompt $\eta_c(1S)$ cross-sections in this kinematic

region are determined to be

$$(\sigma_{\eta_c(1S)})_{\sqrt{s}=7\,\text{TeV}} = 0.52 \pm 0.09 \pm 0.08 \pm 0.06_{\sigma_{J/\psi},\,\mathcal{B}}\ \mu\text{b},$$

for $\sqrt{s} = 7$ TeV, and

$$(\sigma_{\eta_c(1S)})_{\sqrt{s}=8\,\text{TeV}} = 0.59 \pm 0.11 \pm 0.09 \pm 0.08_{\sigma_{J/\psi},\,\mathcal{B}}\ \mu\text{b},$$

for $\sqrt{s} = 8$ TeV. Uncertainties associated with the $J/\psi \to p\bar{p}$ and $\eta_c(1S) \to p\bar{p}$ branching fractions, and with the J/ψ cross-section measurement, are combined into the last uncertainty component, dominated by the knowledge of the branching fractions. This is the first measurement of prompt $\eta_c(1S)$ production in pp collisions. The cross-section for the $\eta_c(1S)$ prompt production is in agreement with the colour-singlet leading order (LO) calculations, while the predicted cross-section exceeds the observed value by two orders of magnitude when the colour-octet LO contribution is taken into account [33]. However, the NLO contribution is expected to significantly modify the LO result [11]. Future measurements at the LHC design energy of $\sqrt{s} = 14$ TeV may allow a study of the energy dependence of the $\eta_c(1S)$ prompt production.

The $\eta_c(1S)$ differential cross-section as a function of p_{T} is obtained by fitting the $p\bar{p}$ invariant mass spectrum in three or four bins of p_{T}. The same procedure as used to extract the $\eta_c(1S)$ cross-section is followed. The J/ψ p_{T} spectrum measured in Refs. [1–3] is used to obtain the $\eta_c(1S)$ p_{T} spectrum for both prompt production and inclusive $\eta_c(1S)$ production in b-hadron decays (Fig. 3). The p_{T} dependence of the $\eta_c(1S)$ production rate exhibits similar behaviour to the J/ψ meson rate in the kinematic region studied.

The performance of the LHCb tracking system and the use of a final state common to J/ψ and $\eta_c(1S)$ decays allows a precise measurement of the mass difference between the two mesons. In order to measure the $\eta_c(1S)$ mass relative to the well-reconstructed and well-known J/ψ mass, a momentum scale calibration [34] is applied on data, and validated with the J/ψ mass measurement. The $M_{J/\psi}$ and $\Delta M_{J/\psi,\,\eta_c(1S)}$ values are extracted from the fit to the $p\bar{p}$ invariant mass in the low-background sample of charmonium candidates produced in b-hadron decays (Fig. 1). The J/ψ mass measurement, $M_{J/\psi} = 3096.66 \pm 0.19 \pm 0.02\,\text{MeV}/c^2$, agrees well with the average from Ref. [21]. The mass difference is measured to be

$$\Delta M_{J/\psi,\,\eta_c(1S)} = 114.7 \pm 1.5 \pm 0.1\,\text{MeV}/c^2.$$

The systematic uncertainty is dominated by the parametrization of the $J/\psi \to p\bar{p}\pi^0$ contribution. The mass difference agrees with the average from Ref. [21]. In addition, the $\eta_c(1S)$ natural width is obtained from the fit to the $p\bar{p}$ invariant mass (Fig. 1), $\Gamma_{\eta_c(1S)} = 25.8 \pm 5.2 \pm 1.9\,\text{MeV}$. The systematic uncertainty is dominated by knowledge of the detector mass resolution. The value of $\Gamma_{\eta_c(1S)}$ obtained is in good agreement with the average from Ref. [21], but it is less precise than previous measurements.

6 Summary

In summary, $\eta_c(1S)$ production is studied using pp collision data corresponding to integrated luminosities of $0.7\,\text{fb}^{-1}$ and $2.0\,\text{fb}^{-1}$, collected at centre-of-mass energies $\sqrt{s} = 7$ TeV and $\sqrt{s} = 8$ TeV, respectively. The inclusive branching fraction of b-hadron decays into $\eta_c(1S)$ mesons with $p_{\text{T}} > 6.5\,\text{GeV}/c$, relative to the corresponding fraction into J/ψ mesons, is measured, for the first time, to be

$$\mathcal{B}(b \to \eta_c(1S)X)/\mathcal{B}(b \to J/\psi X) = 0.421 \pm 0.055 \pm 0.025 \pm 0.045_{\mathcal{B}}.$$

The first uncertainty is statistical, the second is systematic, and the third is due to uncertainties in the branching fractions of $\eta_c(1S)$ and J/ψ meson decays to the $p\bar{p}$ final state. The inclusive branching fraction of b-hadrons into $\eta_c(1S)$ mesons is derived as

$$\mathcal{B}(b \to \eta_c(1S)X) = (4.88 \pm 0.64 \pm 0.29 \pm 0.67_{\mathcal{B}}) \times 10^{-3},$$

where the third uncertainty component includes also the uncertainty on the inclusive branching fraction of b-hadrons into J/ψ mesons. The $\eta_c(1S)$ prompt production cross-section in the kinematic region $2.0 < y < 4.5$ and $p_{\text{T}} > 6.5\,\text{GeV}/c$, relative to the corresponding J/ψ meson cross-section, is measured, for the first time, to be

$$(\sigma_{\eta_c(1S)}/\sigma_{J/\psi})_{\sqrt{s}=7\,\text{TeV}} = 1.74 \pm 0.29 \pm 0.28 \pm 0.18_{\mathcal{B}},$$
$$(\sigma_{\eta_c(1S)}/\sigma_{J/\psi})_{\sqrt{s}=8\,\text{TeV}} = 1.60 \pm 0.29 \pm 0.25 \pm 0.17_{\mathcal{B}},$$

where the third uncertainty component is due to uncertainties in the branching fractions of $\eta_c(1S)$ and J/ψ meson decays to the $p\bar{p}$ final state. From these measurements, absolute $\eta_c(1S)$ prompt cross-sections are derived, yielding

$$(\sigma_{\eta_c(1S)})_{\sqrt{s}=7\,\text{TeV}} = 0.52 \pm 0.09 \pm 0.08 \pm 0.06_{\sigma_{J/\psi},\,\mathcal{B}}\ \mu\text{b},$$
$$(\sigma_{\eta_c(1S)})_{\sqrt{s}=8\,\text{TeV}} = 0.59 \pm 0.11 \pm 0.09 \pm 0.08_{\sigma_{J/\psi},\,\mathcal{B}}\ \mu\text{b},$$

where the third uncertainty includes an additional contribution from the J/ψ meson cross-section. The above results assume that the J/ψ is unpolarized. The $\eta_c(1S)$ prompt cross-section is in agreement with the colour-singlet LO calculations, whereas the colour-octet LO contribution predicts a cross-section that exceeds the observed value by two orders of magnitude [33]. The p_{T} dependences of the $\eta_c(1S)$ and J/ψ production rates exhibit similar behaviour in the kinematic region studied. The difference between the J/ψ and $\eta_c(1S)$ meson masses is also measured, yielding $\Delta M_{J/\psi,\,\eta_c(1S)} = 114.7 \pm 1.5 \pm 0.1\,\text{MeV}/c^2$, where the first uncertainty is statistical and the second is systematic. The result is consistent with the average from Ref. [21].

Acknowledgments We would like to thank Emi Kou for motivating the studies of charmonium production in LHCb using hadronic final states and the useful discussions regarding charmonium production mechanisms. We express our gratitude to our colleagues in the CERN accelerator departments for the excellent performance of the LHC. We thank the technical and administrative staff at the LHCb institutes. We acknowledge support from CERN and from the national agencies: CAPES, CNPq, FAPERJ and FINEP (Brazil); NSFC (China); CNRS/IN2P3 (France); BMBF, DFG, HGF and MPG (Germany); SFI (Ireland); INFN (Italy); FOM and NWO (The Netherlands); MNiSW and NCN (Poland); MEN/IFA (Romania); MinES and FANO (Russia); MinECo (Spain); SNSF and SER (Switzerland); NASU (Ukraine); STFC (United Kingdom); NSF (USA). The Tier1 computing centres are supported by IN2P3 (France), KIT and BMBF (Germany), INFN (Italy), NWO and SURF (The Netherlands), PIC (Spain), GridPP (United Kingdom). We are indebted to the communities behind the multiple open source software packages on which we depend. We are also thankful for the computing resources and the access to software R&D tools provided by Yandex LLC (Russia). Individual groups or members have received support from EPLANET, Marie Skłodowska-Curie Actions and ERC (European Union), Conseil général de Haute-Savoie, Labex ENIGMASS and OCEVU, Région Auvergne (France), RFBR (Russia), XuntaGal and GENCAT (Spain), Royal Society and Royal Commission for the Exhibition of 1851 (United Kingdom).

Funded by SCOAP[3].

References

1. LHCb collaboration, R. Aaij et al., Measurement of J/ψ production in pp collisions at $\sqrt{s} = 7$ TeV. Eur. Phys. J. C **71**, 1645 (2011). arXiv:1103.0423
2. LHCb collaboration, R. Aaij et al., Measurement of J/ψ polarization in pp collisions at $\sqrt{s} = 7$ TeV. Eur. Phys. J. C **73**, 2631 (2013). arXiv:1307.6379
3. LHCb collaboration, R. Aaij et al., Production of J/ψ and Υ mesons in pp collisions at $\sqrt{s} = 8$ TeV. JHEP **06**, 064 (2013). arXiv:1304.6977
4. CMS collaboration, S. Chatrchyan et al., J/ψ and $\psi(2S)$ production in pp collisions at $\sqrt{s} = 7$TeV. JHEP **02**, 011 (2012). arXiv:1111.1557
5. ATLAS collaboration, G. Aad et al., Measurement of the differential cross-sections of inclusive, prompt and non-prompt J/ψ production in proton–proton collisions at $\sqrt{s} = 7$TeV. Nucl. Phys. B **850**, 387 (2011). arXiv:1104.3038
6. ALICE collaboration, B. Abelev et al., Measurement of prompt J/ψ and beauty hadron production cross sections at mid-rapidity in pp collisions at $\sqrt{s} = 7$TeV. JHEP **11**, 065 (2012). arXiv:1205.5880
7. Y.-Q. Ma, K. Wang, K.-T. Chao, J/ψ (ψ') production at the Tevatron and LHC at $O(\alpha_s^4 v^4)$ in nonrelativistic QCD. Phys. Rev. Lett. **106**, 042002 (2011). arXiv:1009.3655
8. N. Brambilla et al., Heavy quarkonium: progress, puzzles, and opportunities. Eur. Phys. J. C **71**, 1534 (2011). arXiv:1010.5827
9. M. Butenschoen, B.A. Kniehl, J/ψ polarization at the Tevatron and the LHC: nonrelativistic-QCD factorization at the crossroads. Phys. Rev. Lett. **108**, 172002 (2012). arXiv:1201.1872
10. K.-T. Chao et al., J/ψ polarization at hadron colliders in nonrelativistic QCD. Phys. Rev. Lett. **108**, 242004 (2012). arXiv:1201.2675
11. F. Maltoni, A. Polosa, Observation potential for η_b at the Fermilab Tevatron. Phys. Rev. D **70**, 054014 (2004). arXiv:hep-ph/0405082
12. A. Petrelli et al., NLO production and decay of quarkonium. Nucl. Phys. B **514**, 245 (1998). arXiv:hep-ph/9707223
13. J.H. Kühn, E. Mirkes, QCD corrections to toponium production at hadron colliders. Phys. Rev. D **48**, 179 (1993). arXiv:hep-ph/9301204
14. LHCb collaboration, R. Aaij et al., Measurement of the relative rate of prompt χ_{c0}, χ_{c1} and χ_{c2} production at $\sqrt{s} = 7$ TeV. JHEP **10**, 115 (2013). arXiv:1307.4285
15. CLEO collaboration, R. Balest et al., Inclusive decays of B mesons to charmonium. Phys. Rev. D **52**, 2661 (1995)
16. BaBar Collaboration,B. Aubert et al., Measurement of the $B^+ \to p\bar{p}K^+$ branching fraction and study of the decay dynamics. Phys. Rev. D **72**, 051101 (2005). arXiv:hep-ex/0507012
17. BELLE Collaboration, J. Wei et al., Study of $B^+ \to p\bar{p}K^+$ and $B^+ \to p\bar{p}\pi^+$. Phys. Lett. B **659**, 80 (2008). arXiv:0706.4167
18. LHCb collaboration, R. Aaij et al., Measurements of the branching fractions of $B^+ \to p\bar{p}K^+$ decays. Eur. Phys. J. C **73**, 2462 (2013). arXiv:1303.7133
19. LHCb collaboration, R. Aaij et al., Measurement of $\psi(2S)$ meson production in pp collisions at $\sqrt{s} = 7$ TeV. Eur. Phys. J. C **72**, 2100 (2012). arXiv:1204.1258
20. S. Barsuk, J. He, E. Kou, B. Viaud, Investigating charmonium production at LHC with the $p\bar{p}$ final state. Phys. Rev. D **86**, 034011 (2012). arXiv:1202.2273
21. Particle Data Group,K. Olive et al., Review of particle physics. Chin. Phys. C **38**, 090001 (2014)
22. BESIII collaboration, M. Ablikim et al., Measurements of the mass and width of the η_c using $\psi' \to \gamma\eta_c$. Phys. Rev. Lett. **108**, 222002 (2012). arXiv:1111.0398
23. BESIII collaboration, M. Ablikim et al., Study of $\psi(3686) \to \pi^0 h_c$, $h_c \to \gamma\eta_c$ via η_c exclusive decays. Phys. Rev. D **86**, 092009 (2012). arXiv:1209.4963
24. LHCb collaboration, A.A. Alves Jr. et al., The LHCb detector at the LHC. JINST **3**, S08005 (2008)
25. M. Adinolfi et al., Performance of the LHCb RICH detector at the LHC. Eur. Phys. J. C **73**, 2431 (2013). arXiv:1211.6759
26. T. Sjöstrand, S. Mrenna, P. Skands, PYTHIA 6.4 physics and manual. JHEP **05**, 026 (2006). arXiv:hep-ph/0603175
27. I. Belyaev et al., Handling of the generation of primary events in Gauss, the LHCb simulation framework. J. Phys. Conf. Ser. **331**, 032047 (2011)
28. D.J. Lange, The EvtGen particle decay simulation package. Nucl. Instrum. Methods **A462**, 152 (2001)
29. P. Golonka, Z. Was, PHOTOS Monte Carlo: A precision tool for QED corrections in Z and W decays. Eur. Phys. J. C **45**, 97 (2006). arXiv:hep-ph/0506026
30. Geant4 collaboration, J. Allison et al., Geant4 developments and applications. IEEE Trans. Nucl. Sci. **53**, 270 (2006)
31. Geant4 collaboration, S. Agostinelli et al., Geant4: a simulation toolkit. Nucl. Instrum. Methods A **506**, 250 (2003)
32. M. Clemencic et al., The LHCb simulation application, Gauss: design, evolution and experience. J. Phys. Conf. Ser. **331**, 032023 (2011)
33. S.S. Biswal, K. Sridhar, η_c production at the large hadron collider. J. Phys. G **39**, 015008 (2012). arXiv:1007.5163
34. LHCb collaboration, R. Aaij et al., Measurement of the Λ_b^0, Ξ_b^- and Ω_b^- baryon masses. Phys. Rev. Lett. **110**, 182001 (2013). arXiv:1302.1072

LHCb Collaboration

R. Aaij[41], C. Abellán Beteta[40], B. Adeva[37], M. Adinolfi[46], A. Affolder[52], Z. Ajaltouni[5], S. Akar[6], J. Albrecht[9], F. Alessio[38], M. Alexander[51], S. Ali[41], G. Alkhazov[30], P. Alvarez Cartelle[37], A. A. Alves Jr[25,38], S. Amato[2], S. Amerio[22], Y. Amhis[7], L. An[3], L. Anderlini[17,g], J. Anderson[40], R. Andreassen[57], M. Andreotti[16,f], J. E. Andrews[58], R. B. Appleby[54], O. Aquines Gutierrez[10], F. Archilli[38], A. Artamonov[35], M. Artuso[59], E. Aslanides[6], G. Auriemma[25,n], M. Baalouch[5], S. Bachmann[11], J. J. Back[48], A. Badalov[36], C. Baesso[60], W. Baldini[16], R. J. Barlow[54], C. Barschel[38], S. Barsuk[7], W. Barter[47], V. Batozskaya[28], V. Battista[39], A. Bay[39], L. Beaucourt[4], J. Beddow[51], F. Bedeschi[23], I. Bediaga[1], S. Belogurov[31], K. Belous[35], I. Belyaev[31], E. Ben-Haim[8], G. Bencivenni[18], S. Benson[38], J. Benton[46], A. Berezhnoy[32], R. Bernet[40], M.-O. Bettler[47], M. van Beuzekom[41], A. Bien[11], S. Bifani[45], T. Bird[54], A. Bizzeti[17,i], P. M. Bjørnstad[54], T. Blake[48], F. Blanc[39], J. Blouw[10], S. Blusk[59], V. Bocci[25], A. Bondar[34], N. Bondar[30,38], W. Bonivento[15,38], S. Borghi[54], A. Borgia[59], M. Borsato[7], T. J. V. Bowcock[52], E. Bowen[40], C. Bozzi[16], T. Brambach[9], J. Bressieux[39], D. Brett[54], M. Britsch[10], T. Britton[59], J. Brodzicka[54], N. H. Brook[46], H. Brown[52], A. Bursche[40], G. Busetto[22,r], J. Buytaert[38], S. Cadeddu[15], R. Calabrese[16,f], M. Calvi[20,k], M. Calvo Gomez[36,p], P. Campana[18,38], D. Campora Perez[38], A. Carbone[14,d], G. Carboni[24,l], R. Cardinale[19,38,j], A. Cardini[15], L. Carson[50], K. Carvalho Akiba[2], G. Casse[52], L. Cassina[20], L. Castillo Garcia[38], M. Cattaneo[38], Ch. Cauet[9], R. Cenci[58], M. Charles[8], Ph. Charpentier[38], M. Chefdeville[4], S. Chen[54], S.-F. Cheung[55], N. Chiapolini[40], M. Chrzaszcz[26,40], K. Ciba[38], X. Cid Vidal[38], G. Ciezarek[53], P. E. L. Clarke[50], M. Clemencic[38], H. V. Cliff[47], J. Closier[38], V. Coco[38], J. Cogan[6], E. Cogneras[5], V. Cogoni[15], L. Cojocariu[29], P. Collins[38], A. Comerma-Montells[11], A. Contu[15,38], A. Cook[46], M. Coombes[46], S. Coquereau[8], G. Corti[38], M. Corvo[16,f], I. Counts[56], B. Couturier[38], G. A. Cowan[50], D. C. Craik[48], M. Cruz Torres[60], S. Cunliffe[53], R. Currie[50], C. D'Ambrosio[38], J. Dalseno[46], P. David[8], P. N. Y. David[41], A. Davis[57], K. De Bruyn[41], S. De Capua[54], M. De Cian[11], J. M. De Miranda[1], L. De Paula[2], W. De Silva[57], P. De Simone[18], D. Decamp[4], M. Deckenhoff[9], L. Del Buono[8], N. Déléage[4], D. Derkach[55], O. Deschamps[5], F. Dettori[38], A. Di Canto[38], H. Dijkstra[38], S. Donleavy[52], F. Dordei[11], M. Dorigo[39], A. Dosil Suárez[37], D. Dossett[48], A. Dovbnya[43], K. Dreimanis[52], G. Dujany[54], F. Dupertuis[39], P. Durante[38], R. Dzhelyadin[35], A. Dziurda[26], A. Dzyuba[30], S. Easo[38,49], U. Egede[53], V. Egorychev[31], S. Eidelman[34], S. Eisenhardt[50], U. Eitschberger[9], R. Ekelhof[9], L. Eklund[51], I. El Rifai[5], E. Elena[40], Ch. Elsasser[40], S. Ely[59], S. Esen[11], H.-M. Evans[47], T. Evans[55], A. Falabella[14], C. Färber[11], C. Farinelli[41], N. Farley[45], S. Farry[52], R. F. Fay[52], D. Ferguson[50], V. Fernandez Albor[37], F. Ferreira Rodrigues[1], M. Ferro-Luzzi[38], S. Filippov[33], M. Fiore[16,f], M. Fiorini[16,f], M. Firlej[27], C. Fitzpatrick[39], T. Fiutowski[27], P. Fol[53], M. Fontana[10], F. Fontanelli[19,j], R. Forty[38], O. Francisco[2], M. Frank[38], C. Frei[38], M. Frosini[17,g], J. Fu[21,38], E. Furfaro[24,l], A. Gallas Torreira[37], D. Galli[14,d], S. Gallorini[22,38], S. Gambetta[19,j], M. Gandelman[2], P. Gandini[59], Y. Gao[3], J. García Pardiñas[37], J. Garofoli[59], J. Garra Tico[47], L. Garrido[36], C. Gaspar[38], R. Gauld[55], L. Gavardi[9], G. Gavrilov[30], A. Geraci[21,v], E. Gersabeck[11], M. Gersabeck[54], T. Gershon[48], Ph. Ghez[4], A. Gianelle[22], S. Gianì[39], V. Gibson[47], L. Giubega[29], V. V. Gligorov[38], C. Göbel[60], D. Golubkov[31], A. Golutvin[31,38,53], A. Gomes[1,a], C. Gotti[20], M. Grabalosa Gándara[5], R. Graciani Diaz[36], L. A. Granado Cardoso[38], E. Graugés[36], G. Graziani[17], A. Grecu[29], E. Greening[55], S. Gregson[47], P. Griffith[45], L. Grillo[11], O. Grünberg[62], B. Gui[59], E. Gushchin[33], Yu. Guz[35,38], T. Gys[38], C. Hadjivasiliou[59], G. Haefeli[39], C. Haen[38], S. C. Haines[47], S. Hall[53], B. Hamilton[58], T. Hampson[46], X. Han[11], S. Hansmann-Menzemer[11], N. Harnew[55], S. T. Harnew[46], J. Harrison[54], J. He[38], T. Head[38], V. Heijne[41], K. Hennessy[52], P. Henrard[5], L. Henry[8], J. A. Hernando Morata[37], E. van Herwijnen[38], M. Heß[62], A. Hicheur[2], D. Hill[55], M. Hoballah[5], C. Hombach[54], W. Hulsbergen[41], P. Hunt[55], N. Hussain[55], D. Hutchcroft[52], D. Hynds[51], M. Idzik[27], P. Ilten[56], R. Jacobsson[38], A. Jaeger[11], J. Jalocha[55], E. Jans[41], P. Jaton[39], A. Jawahery[58], F. Jing[3], M. John[55], D. Johnson[38], C. R. Jones[47], C. Joram[38], B. Jost[38], N. Jurik[59], M. Kaballo[9], S. Kandybei[43], W. Kanso[6], M. Karacson[38], T. M. Karbach[38], S. Karodia[51], M. Kelsey[59], I. R. Kenyon[45], T. Ketel[42], B. Khanji[20], C. Khurewathanakul[39], S. Klaver[54], K. Klimaszewski[28], O. Kochebina[7], M. Kolpin[11], I. Komarov[39], R. F. Koopman[42], P. Koppenburg[38,41], M. Korolev[32], A. Kozlinskiy[41], L. Kravchuk[33], K. Kreplin[11], M. Kreps[48], G. Krocker[11], P. Krokovny[34], F. Kruse[9], W. Kucewicz[26,o], M. Kucharczyk[20,26,k], V. Kudryavtsev[34], K. Kurek[28], T. Kvaratskheliya[31], V. N. La Thi[39], D. Lacarrere[38], G. Lafferty[54], A. Lai[15], D. Lambert[50], R. W. Lambert[42], G. Lanfranchi[18], C. Langenbruch[48], B. Langhans[38], T. Latham[48], C. Lazzeroni[45], R. Le Gac[6], J. van Leerdam[41], J.-P. Lees[4], R. Lefèvre[5], A. Leflat[32], J. Lefrançois[7], S. Leo[23], O. Leroy[6], T. Lesiak[26], B. Leverington[11], Y. Li[3], T. Likhomanenko[63], M. Liles[52], R. Lindner[38], C. Linn[38], F. Lionetto[40], B. Liu[15], S. Lohn[38], I. Longstaff[51], J. H. Lopes[2], N. Lopez-March[39], P. Lowdon[40], D. Lucchesi[22,r], H. Luo[50], A. Lupato[22], E. Luppi[16,f], O. Lupton[55], F. Machefert[7], I. V. Machikhiliyan[31], F. Maciuc[29], O. Maev[30], S. Malde[55], A. Malinin[63], G. Manca[15,e], G. Mancinelli[6], A. Mapelli[38], J. Maratas[5], J.F. Marchand[4], U. Marconi[14], C. Marin Benito[36], P. Marino[23,t], R. Märki[39], J. Marks[11], G. Martellotti[25], A. Martens[8], A. Martín Sánchez[7], M. Martinelli[39], D. Martinez Santos[38,42], F. Martinez Vidal[64], D. Martins Tostes[2], A. Massafferri[1], R. Matev[38], Z. Mathe[38], C. Matteuzzi[20], A. Mazurov[45],

M. McCann[53], J. McCarthy[45], A. McNab[54], R. McNulty[12], B. McSkelly[52], B. Meadows[57], F. Meier[9], M. Meissner[11], M. Merk[41], D. A. Milanes[8], M.-N. Minard[4], N. Moggi[14], J. Molina Rodriguez[60], S. Monteil[5], M. Morandin[22], P. Morawski[27], A. Mordà[6], M. J. Morello[23,t], J. Moron[27], A.-B. Morris[50], R. Mountain[59], F. Muheim[50], K. Müller[40], M. Mussini[14], B. Muster[39], P. Naik[46], T. Nakada[39], R. Nandakumar[49], I. Nasteva[2], M. Needham[50], N. Neri[21], S. Neubert[38], N. Neufeld[38], M. Neuner[11], A. D. Nguyen[39], T. D. Nguyen[39], C. Nguyen-Mau[39,q], M. Nicol[7], V. Niess[5], R. Niet[9], N. Nikitin[32], T. Nikodem[11], A. Novoselov[35], D. P. O'Hanlon[48], A. Oblakowska-Mucha[27,38], V. Obraztsov[35], S. Oggero[41], S. Ogilvy[51], O. Okhrimenko[44], R. Oldeman[15,e], G. Onderwater[65], M. Orlandea[29], J. M. Otalora Goicochea[2], P. Owen[53], A. Oyanguren[64], B. K. Pal[59], A. Palano[13,c], F. Palombo[21,u], M. Palutan[18], J. Panman[38], A. Papanestis[38,49], M. Pappagallo[51], L. L. Pappalardo[16,f], C. Parkes[54], C. J. Parkinson[9,45], G. Passaleva[17], G. D. Patel[52], M. Patel[53], C. Patrignani[19,j], A. Pazos Alvarez[37], A. Pearce[54], A. Pellegrino[41], M. Pepe Altarelli[38], S. Perazzini[14,d], E. Perez Trigo[37], P. Perret[5], M. Perrin-Terrin[6], L. Pescatore[45], E. Pesen[66], K. Petridis[53], A. Petrolini[19,j], E. Picatoste Olloqui[36], B. Pietrzyk[4], T. Pilař[48], D. Pinci[25], A. Pistone[19], S. Playfer[50], M. Plo Casasus[37], F. Polci[8], A. Poluektov[34,48], E. Polycarpo[2], A. Popov[35], D. Popov[10], B. Popovici[29], C. Potterat[2], E. Price[46], J.D. Price[52], J. Prisciandaro[39], A. Pritchard[52], C. Prouve[46], V. Pugatch[44], A. Puig Navarro[39], G. Punzi[23,s], W. Qian[4], B. Rachwal[26], J. H. Rademacker[46], B. Rakotomiaramanana[39], M. Rama[18], M. S. Rangel[2], I. Raniuk[43], N. Rauschmayr[38], G. Raven[42], F. Redi[53], S. Reichert[54], M. M. Reid[48], A. C. dos Reis[1], S. Ricciardi[49], S. Richards[46], M. Rihl[38], K. Rinnert[52], V. Rives Molina[36], P. Robbe[7], A. B. Rodrigues[1], E. Rodrigues[54], P. Rodriguez Perez[54], S. Roiser[38], V. Romanovsky[35], A. Romero Vidal[37], M. Rotondo[22], J. Rouvinet[39], T. Ruf[38], H. Ruiz[36], P. Ruiz Valls[64], J. J. Saborido Silva[37], N. Sagidova[30], P. Sail[51], B. Saitta[15,e], V. Salustino Guimaraes[2], C. Sanchez Mayordomo[64], B. Sanmartin Sedes[37], R. Santacesaria[25], C. Santamarina Rios[37], E. Santovetti[24,l], A. Sarti[18,m], C. Satriano[25,n], A. Satta[24], D.M. Saunders[46], M. Savrie[16,f], D. Savrina[31,32], M. Schiller[42], H. Schindler[38], M. Schlupp[9], M. Schmelling[10], B. Schmidt[38], O. Schneider[39], A. Schopper[38], M.-H. Schune[7], R. Schwemmer[38], B. Sciascia[18], A. Sciubba[25], M. Seco[37], A. Semennikov[31], I. Sepp[53], N. Serra[40], J. Serrano[6], L. Sestini[22], P. Seyfert[11], M. Shapkin[35], I. Shapoval[16,43,f], Y. Shcheglov[30], T. Shears[52], L. Shekhtman[34], V. Shevchenko[63], A. Shires[9], R. Silva Coutinho[48], G. Simi[22], M. Sirendi[47], N. Skidmore[46], T. Skwarnicki[59], N. A. Smith[52], E. Smith[49,55], E. Smith[53], J. Smith[47], M. Smith[54], H. Snoek[41], M. D. Sokoloff[57], F. J. P. Soler[51], F. Soomro[39], D. Souza[46], B. Souza De Paula[2], B. Spaan[9], A. Sparkes[50], P. Spradlin[51], S. Sridharan[38], F. Stagni[38], M. Stahl[11], S. Stahl[11], O. Steinkamp[40], O. Stenyakin[35], S. Stevenson[55], S. Stoica[29], S. Stone[59], B. Storaci[40], S. Stracka[23], M. Straticiuc[29], U. Straumann[40], R. Stroili[22], V. K. Subbiah[38], L. Sun[57], W. Sutcliffe[53], K. Swientek[27], S. Swientek[9], V. Syropoulos[42], M. Szczekowski[28], P. Szczypka[38,39], D. Szilard[2], T. Szumlak[27], S. T'Jampens[4], M. Teklishyn[7], G. Tellarini[16,f], F. Teubert[38], C. Thomas[55], E. Thomas[38], J. van Tilburg[41], V. Tisserand[4], M. Tobin[39], S. Tolk[42], L. Tomassetti[16,f], D. Tonelli[38], S. Topp-Joergensen[55], N. Torr[55], E. Tournefier[4], S. Tourneur[39], M. T. Tran[39], M. Tresch[40], A. Tsaregorodtsev[6], P. Tsopelas[41], N. Tuning[41], M. Ubeda Garcia[38], A. Ukleja[28], A. Ustyuzhanin[63], U. Uwer[11], C. Vacca[15], V. Vagnoni[14], G. Valenti[14], A. Vallier[7], R. Vazquez Gomez[18], P. Vazquez Regueiro[37], C. Vázquez Sierra[37], S. Vecchi[16], J. J. Velthuis[46], M. Veltri[17,h], G. Veneziano[39], M. Vesterinen[11], B. Viaud[7], D. Vieira[2], M. Vieites Diaz[37], X. Vilasis-Cardona[36,p], A. Vollhardt[40], D. Volyanskyy[10], D. Voong[46], A. Vorobyev[30], V. Vorobyev[34], C. Voß[62], H. Voss[10], J. A. de Vries[41], R. Waldi[62], C. Wallace[48], R. Wallace[12], J. Walsh[23], S. Wandernoth[11], J. Wang[59], D. R. Ward[47], N. K. Watson[45], D. Websdale[53], M. Whitehead[48], J. Wicht[38], D. Wiedner[11], G. Wilkinson[38,55], M. P. Williams[45], M. Williams[56], H.W. Wilschut[65], F. F. Wilson[49], J. Wimberley[58], J. Wishahi[9], W. Wislicki[28], M. Witek[26], G. Wormser[7], S. A. Wotton[47], S. Wright[47], K. Wyllie[38], Y. Xie[61], Z. Xing[59], Z. Xu[39], Z. Yang[3], X. Yuan[3], O. Yushchenko[35], M. Zangoli[14], M. Zavertyaev[10,b], L. Zhang[59], W. C. Zhang[12], Y. Zhang[3], A. Zhelezov[11], A. Zhokhov[31], L. Zhong[3], A. Zvyagin[38]

[1] Centro Brasileiro de Pesquisas Físicas (CBPF), Rio de Janeiro, Brazil
[2] Universidade Federal do Rio de Janeiro (UFRJ), Rio de Janeiro, Brazil
[3] Center for High Energy Physics, Tsinghua University, Beijing, China
[4] LAPP, Université de Savoie, CNRS/IN2P3, Annecy-Le-Vieux, France
[5] LPC, Clermont Université, Université Blaise Pascal, CNRS/IN2P3, Clermont-Ferrand, France
[6] CPPM, Aix-Marseille Université, CNRS/IN2P3, Marseille, France
[7] LAL, Université Paris-Sud, CNRS/IN2P3, Orsay, France
[8] LPNHE, Université Pierre et Marie Curie, Université Paris Diderot, CNRS/IN2P3, Paris, France
[9] Fakultät Physik, Technische Universität Dortmund, Dortmund, Germany
[10] Max-Planck-Institut für Kernphysik (MPIK), Heidelberg, Germany
[11] Physikalisches Institut, Ruprecht-Karls-Universität Heidelberg, Heidelberg, Germany
[12] School of Physics, University College Dublin, Dublin, Ireland

[13] Sezione INFN di Bari, Bari, Italy
[14] Sezione INFN di Bologna, Bologna, Italy
[15] Sezione INFN di Cagliari, Cagliari, Italy
[16] Sezione INFN di Ferrara, Ferrara, Italy
[17] Sezione INFN di Firenze, Florence, Italy
[18] Laboratori Nazionali dell'INFN di Frascati, Frascati, Italy
[19] Sezione INFN di Genova, Genoa, Italy
[20] Sezione INFN di Milano Bicocca, Milan, Italy
[21] Sezione INFN di Milano, Milan, Italy
[22] Sezione INFN di Padova, Padua, Italy
[23] Sezione INFN di Pisa, Pisa, Italy
[24] Sezione INFN di Roma Tor Vergata, Rome, Italy
[25] Sezione INFN di Roma La Sapienza, Rome, Italy
[26] Henryk Niewodniczanski Institute of Nuclear Physics, Polish Academy of Sciences, Kraków, Poland
[27] Faculty of Physics and Applied Computer Science, AGH-University of Science and Technology, Kraków, Poland
[28] National Center for Nuclear Research (NCBJ), Warsaw, Poland
[29] Horia Hulubei National Institute of Physics and Nuclear Engineering, Bucharest-Magurele, Romania
[30] Petersburg Nuclear Physics Institute (PNPI), Gatchina, Russia
[31] Institute of Theoretical and Experimental Physics (ITEP), Moscow, Russia
[32] Institute of Nuclear Physics, Moscow State University (SINP MSU), Moscow, Russia
[33] Institute for Nuclear Research of the Russian Academy of Sciences (INR RAN), Moscow, Russia
[34] Budker Institute of Nuclear Physics (SB RAS) and Novosibirsk State University, Novosibirsk, Russia
[35] Institute for High Energy Physics (IHEP), Protvino, Russia
[36] Universitat de Barcelona, Barcelona, Spain
[37] Universidad de Santiago de Compostela, Santiago de Compostela, Spain
[38] European Organization for Nuclear Research (CERN), Geneva, Switzerland
[39] Ecole Polytechnique Fédérale de Lausanne (EPFL), Lausanne, Switzerland
[40] Physik-Institut, Universität Zürich, Zurich, Switzerland
[41] Nikhef National Institute for Subatomic Physics, Amsterdam, The Netherlands
[42] Nikhef National Institute for Subatomic Physics, VU University Amsterdam, Amsterdam, The Netherlands
[43] NSC Kharkiv Institute of Physics and Technology (NSC KIPT), Kharkiv, Ukraine
[44] Institute for Nuclear Research of the National Academy of Sciences (KINR), Kyiv, Ukraine
[45] University of Birmingham, Birmingham, UK
[46] H.H. Wills Physics Laboratory, University of Bristol, Bristol, UK
[47] Cavendish Laboratory, University of Cambridge, Cambridge, UK
[48] Department of Physics, University of Warwick, Coventry, UK
[49] STFC Rutherford Appleton Laboratory, Didcot, UK
[50] School of Physics and Astronomy, University of Edinburgh, Edinburgh, UK
[51] School of Physics and Astronomy, University of Glasgow, Glasgow, UK
[52] Oliver Lodge Laboratory, University of Liverpool, Liverpool, UK
[53] Imperial College London, London, UK
[54] School of Physics and Astronomy, University of Manchester, Manchester, UK
[55] Department of Physics, University of Oxford, Oxford, UK
[56] Massachusetts Institute of Technology, Cambridge, MA, USA
[57] University of Cincinnati, Cincinnati, OH, USA
[58] University of Maryland, College Park, MD, USA
[59] Syracuse University, Syracuse, NY, USA
[60] Pontifícia Universidade Católica do Rio de Janeiro (PUC-Rio), Rio de Janeiro, Brazil, associated to[2]
[61] Institute of Particle Physics, Central China Normal University, Wuhan, Hubei, China, associated to[3]
[62] Institut für Physik, Universität Rostock, Rostock, Germany, associated to[11]
[63] National Research Centre Kurchatov Institute, Moscow, Russia, associated to[31]
[64] Instituto de Fisica Corpuscular (IFIC), Universitat de Valencia-CSIC, Valencia, Spain, associated to[36]
[65] KVI, University of Groningen, Groningen, The Netherlands, associated to[41]

[66] Celal Bayar University, Manisa, Turkey, associated to[38]

[a] Universidade Federal do Triângulo Mineiro (UFTM), Uberaba, MG, Brazil
[b] P.N. Lebedev Physical Institute, Russian Academy of Science (LPI RAS), Moscow, Russia
[c] Università di Bari, Bari, Italy
[d] Università di Bologna, Bologna, Italy
[e] Università di Cagliari, Cagliari, Italy
[f] Università di Ferrara, Ferrara, Italy
[g] Università di Firenze, Florence, Italy
[h] Università di Urbino, Urbino, Italy
[i] Università di Modena e Reggio Emilia, Modena, Italy
[j] Università di Genova, Genoa, Italy
[k] Università di Milano Bicocca, Milan, Italy
[l] Università di Roma Tor Vergata, Rome, Italy
[m] Università di Roma La Sapienza, Rome, Italy
[n] Università della Basilicata, Potenza, Italy
[o] Faculty of Computer Science, Electronics and Telecommunications, AGH-University of Science and Technology, Kraków, Poland
[p] LIFAELS, La Salle, Universitat Ramon Llull, Barcelona, Spain
[q] Hanoi University of Science, Hanoi, Vietnam
[r] Università di Padova, Padua, Italy
[s] Università di Pisa, Pisa, Italy
[t] Scuola Normale Superiore, Pisa, Italy
[u] Università degli Studi di Milano, Milan, Italy
[v] Politecnico di Milano, Milano, Italy